# *Diagenesis and sedimentary environment of Miocene series in Eboliang III area*

## Guoqiang Sun, Jianguo Yin, Shuncun Zhang, Xinchuan Lu, Shengyin Zhang & Ji#an Shi

Springer

Springer

CrossMark

ORIGINAL ARTICLE

# Diagenesis and sedimentary environment of Miocene series in Eboliang III area

Guoqiang Sun[1] · Jianguo Yin[1,2] · Shuncun Zhang[1] · Xinchuan Lu[1] ·
Shengyin Zhang[1] · Ji′an Shi[1]

**Abstract** This paper presents petrology, mineralogy, and elemental geochemistry research on diagenesis, formation environment, and source material of the Upper Ganchaigou Formation of clastic rocks in the Eboliang III structural belt on the northern margin of the Qaidam basin. Point-line contacts of particles and directional alignment of feldspars show relatively intense compaction. Clays have high content with mean up to 35.03 % of total cement content, mainly consisting of illite, chlorite, and mixed-layer illite–smectite. Carbonate cements contain large amounts of calcite and little dolomite. Carbon and oxygen isotope composition of carbonate cement present $\delta^{13}C$ values between −6.8 and −4.0 ‰ (mean −5.0 ‰) and $\delta^{18}O$ values between −11.1 ‰ and −5.4 ‰ (mean −8.7 ‰). According to $\delta^{13}C$ and $\delta^{18}O$ calculations, ancient salinity Z values are distributed between 108.34 and 114.89 (mean 112.77), and the formation temperature of carbonate cement is between 43.36 and 77.84 °C (mean 62.30 °C). From the analysis of major elements, trace elements, and organic carbon, the diagenetic stage of the Upper Ganchaigou Formation is regarded as the B period of the early diagenesis stage or the A period of the middle diagenesis stage. The sedimentary environment is evolved from dry and cold freshwater and brackish water to warm and wet freshwater during deposition of the Upper Ganchaigou Formation.

## Introduction

Carbonate cements are common diagenetic minerals in various sedimentary clastic rocks (Boles 1998; Abdel-Wahab and McBride 2001; Sun et al. 2002; Rossi et al. 2001). Carbon and oxygen isotope compositions can not only indicate the carbon source (Macaulay et al. 1993; Fayek et al. 2001) and estimate diagenetic temperatures (Friedman and O'Neil 1977), but also distinguish marine and continental environments and provide qualitative information on diagenetic intensity (Zhang 1985). Therefore, research on carbon and oxygen isotope compositions of carbonate cements is valuable in petroleum geology. By analyzing carbon isotopes of authigenic calcite in a sandstone reservoir, Zhu et al. (2007) found that the carbon isotopic variations correlate with $CO_2$ in natural gas and that carbonate cement precipitation and the carbon isotopic composition depend on the thermal evolution of natural gas with $CO_2$; this allowed them to obtain the direction of natural gas transport (N to S) using the carbon isotopes of calcite as a tracer. (Wang et al. 2007a, b) indicated that carbon and oxygen isotope composition of carbonate cements at different formation stages reflect organic–inorganic interactions and source materials in a petroleum reservoir and can act as tracers. Sun et al. (2012) suggested carbonate formation is probably related to organic matter decarboxylation during latest early diagenesis, so that

✉ Guoqiang Sun
sguoqiang@lzb.ac.cn

1 Key Laboratory of Petroleum Resources, Gansu Province/
Key Laboratory of Petroleum Resources Research, Institute
of Geology and Geophysics, Chinese Academy of Sciences,
Lanzhou 730000, People's Republic of China

2 University of Chinese Academy of Sciences, Beijing,
People's Republic of China

Springer

diagenetically produced calcite cement fluids in a sandstone reservoir originate mainly from clast and atmospheric freshwater. Consequently, the function of carbon and oxygen isotope compositions of carbonate cements in identifying formation environment and material source makes them valuable in petroleum geology (Ortoleva 1994; Rosenbaum and Sheppard 1986; Huang et al. 2002; McBride and Parea 2001; Wang et al. 2007a, b; Dong et al. 2004; Zhu et al. 2007; Sun et al. 2012).

The northern fault block belt margin of the Qaidam Basin (NMQB), located south of the Qilian Mountains, is a primary structural unit and contains the Eboliang structural belts, Lenghu structural belt, and the Nanbaxian and Mahai structures (Xie and Guan 2000; Xiao et al. 2005; Sun et al. 2011; Chen et al. 2011; Li et al. 2009). The Eboliang III structural belt is a large-scale structure located in the eastern segment of the Eboliang–Hulu Mountain structural belt in the southern NMQB and is bordered by the Yibei depression, Lenghu Six structural belt, and Lenghu Seven structural belt to the north, the Yiliping depression to the south, the Yikeyawuru and Yahu structures to the east, and Hulu Mountain and Eboliang II structures to the west (Wang et al. 2007a, b; Fig. 1). Given the recent increase in petroleum exploration in the NMQB (Chen and Luo 2004; Liu et al. 2009; Yan et al. 2011; Guo et al. 2011), research on reservoir properties, major controlling factors, diagenetic processes, source materials, and formation environments of target strata have become study foci in this area. However, few studies on reservoir sandstones have been conducted. This study attempts to remedy that by investigating clastic rocks of the Upper Ganchaigou Formation in the Eboliang III structural belt. We used an interdisciplinary approach, including petrology, mineralogy, and elemental geochemistry, to carry out systematic research on diagenesis, diagenetic environment, and source materials to provide additional information for further petroleum exploration.

## Samples and methods

Samples of Upper Ganchaigou Formation clastic rocks were collected from key wells in the Eboliang III structural belt. Preliminary work, such as description and analysis of cores for rock types, rock characteristics, sedimentary structures, and content and composition estimation of carbonate cements, was accomplished before sample collection. Hydrochloric acid (1 % solution) was dropped on the rock in situ. The higher the calcite content in carbonate cement, the more intensive the reaction is (Wang et al. 2007a, b). Microscope, SEM, and X-ray microanalysis ensured that samples used for analysis of carbon and oxygen isotope composition contain solely carbonate cement (Wang et al. 2010). Measurement of carbon and

oxygen isotope composition was carried out with a Thermo Finnigan MAT252 mass spectrometer at the Key Laboratory of Petroleum Resources Research, Institute of Geology and Geophysics, Chinese Academy of Sciences. Minor amount of samples ground to 100–200 mesh were reacted with 100 % orthophosphate at a temperature of 90 °C, and after drying to remove moisture the $CO_2$ produced was tested in the MAT252. Carbon and oxygen isotope compositions of samples were expressed with respect to the Peedee belemnite II standard (PDB II). Major elements, trace elements, and organic carbon analyses were also conducted by the Key Laboratory of Petroleum Resources Research, Institute of Geology and Geophysics, Chinese Academy of Sciences (for detailed methods and procedures refer to lab standard).

## Discussion of results

### Carbonate cement type

Lithology of the Upper Ganchaigou Formation in the Eboliang III structural belt consists mainly of brown sandy mudstone, brownish gray siltstone, grayish-green siltstone, and sandstone. The main carbonate cement is calcite with mean content of up to 12.05 %, according to content analyses of 39 core samples measured by X-ray diffraction. X-ray diffraction analysis was carried out using a Dmax 12kw powder diffractometer (refer to SY/T5163-2010 standard) (Table 1). Minor dolomite was found in only two samples, with mean content of 3.50 %. Microscope observation of 200 thin sections and 100 stained thin sections also demonstrated that calcite is the main carbonate cement with no dolomite (Fig. 2).

### Clay mineral characteristics

The Upper Ganchaigou Formation is buried more than 3000 m deep in the Eboliang III structural belt. Microscope observation of thin sections revealed that particles in sandstone had mainly point-line contacts and that many plastic detritus (such as mica, mudstone, and so on.) show directional alignment (Fig. 3). These phenomena indicate that the rock experienced relatively intense compaction and modification. Clay minerals widely developed in intergranular pores with mean contents of up to 35.03 % of mainly illite, chlorite, kaolinite, and mixed-layer illite–smectite (Fig. 4). Illite was usually thread-like, flaking, or bridging. Chlorite appeared mainly as needle or leaf shapes. Authigenic quartz developed and quartz III overgrowths can be found. According to X-ray diffraction analysis, content of clay minerals varied widely between 11.3 and 54.7 % (mean 35.03 %). The main clay minerals were high maturity illite, chlorite, and mixed-
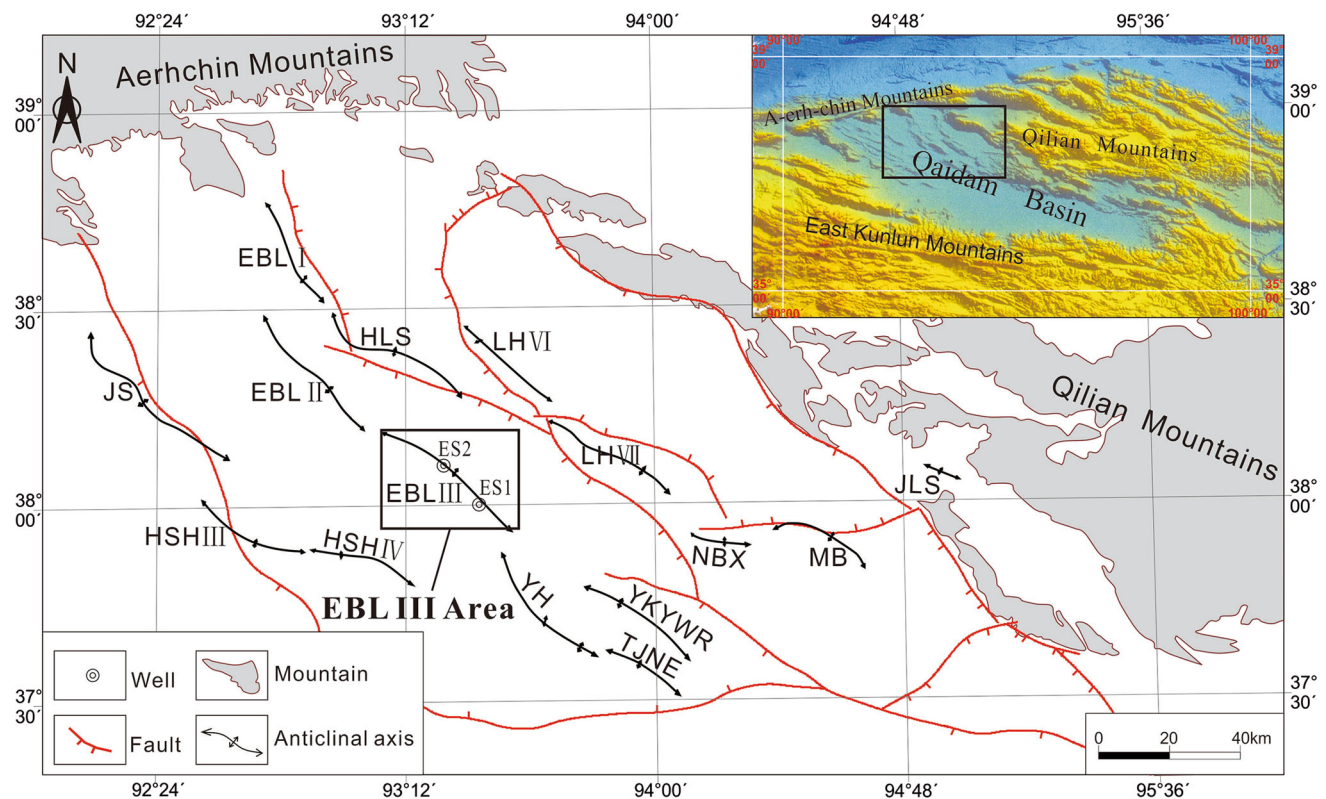
**Fig. 1** Characteristics of the structures in the northern edge of the Qaidam Basin. *LHVI* Lenghu VI, *LHVII* Lenghu VII, *NBX* Nanbaxian, *MB* Mabei, *JLS* Jiulongshan, *JS* Jianshan, *HLS* Hulushan, *EBLI* Eboliang I, *EBLII* Eboliang II, *EBLIII* Eboliang III, *HSHIII* Hongsanhan III, *HSHIV* Hongsanhan IV, *YH* Yau, *TJNE* Taijinaier, *YKYWR* Yikeyawuru

layer illite–smectite (Table 2). Smectite content was high, with a mean of 27.6 % in mixed-layer illite–smectite.

Using the authigenic mineral and carbonate cement characteristics, we identified the diagenetic stage of the Upper Ganchaigou Formation as the B period of the early diagenesis stage/A period of the middle diagenesis stage. This stage was identified from an almost complete absence of smectite, little kaolinite, and a relatively developed mixed-layer of illite–smectite. In the illite–smectite mixed layer, smectite ranges from 25 to 40 % with an average of 27.6 %. Additionally, illite has a needle or thread-like shape, while chlorite shows a mainly needle and leaf appearance. A III-order enlargement of quartz was found and the carbonate cement consists of mainly calcite. The carbonate cement exhibited mainly point-line contacts and mainly primary pores with minor secondary pores.

## Carbon and oxygen isotope composition and source of carbonate cement

Depth, horizon, lithology, and carbon and oxygen isotope composition of the Upper Ganchaigou Formation in the Eboliang III structural belt of the NMQB are listed in Table 1. $\delta^{18}O$ and $\delta^{13}C$ are lighter and range between −11.1 and −5.4 ‰ (mean −8.7 ‰) and −6.8 and −4.0 ‰ (mean −5.0 ‰), respectively. Ancient salinity Z values vary between 108.34 and 114.89 with a mean of 112.77. The deposition temperature of carbonate cement ranges between 43.36 and 77.84 °C with a mean of 62.30 °C. The formation temperature in combination with the above analytical results reinforces our hypothesis that these samples are in the B period of the early diagenesis stage or the A period of the middle diagenesis stage. Organic carbon and carbon in carbonate are natural carbon reservoirs (Cai et al. 2009). Organic carbon is reductive, with depleted $\delta^{13}C$; while carbon in carbonate is oxidative, with enriched $\delta^{13}C$. The $\delta^{18}O$ and $\delta^{13}C$ isotope compositions of carbonates from the study area were used to indicate the formation temperature and environment. $\delta^{18}O$ and $\delta^{13}C$ increase with increased salinity of the formation environment. $\delta^{18}O$ becomes lighter with increased formation temperature. Freshwater leaching and biodegradation during diagenesis can make $\delta^{18}O$ and $\delta^{13}C$ lighter (Liu et al. 2006). $\delta^{13}C$ from organic material is generally light (Zhang et al. 2012). According to the fractionation mechanics of natural carbon (Hudson 1977), $\delta^{13}C$ of inorganic carbon ranges between −4.0 and 4.0 ‰. Lower $\delta^{13}C$ values indicate an effect from organic carbon (Wang et al. 2007a, b).

Table 1 X-ray diffraction analysis of minerals and carbon–oxygen isotopic compositions of Upper Ganchaigou Formation carbonate cements in Eboliang III area

| Well | Horizon | Depth (m) | Lithology | Quartz (%) | Chlorite (%) | Mica (%) | Calcite (%) | Plagioclase (%) | Microcline (%) | Hematite (%) | Dolomite | $\delta^{13}C_{PDB}$ (‰) | $\delta^{18}O_{PDB}$ (‰) | t (°C) | Z |
|---|---|---|---|---|---|---|---|---|---|---|---|---|---|---|---|
| ES1 | $N_1$ | 3615.15 | Brown mudstone | 38 | 19 | 15 | 7 | 14 | 4 | 3 | – | -4.55 | -7.23 | 53.79 | 114.38 |
| ES1 | $N_1$ | 3615.9 | Brown mudstone | 37 | 18 | 15 | 9 | 16 | 3 | 3 | – | -4.91 | -7.82 | 57.27 | 113.35 |
| ES1 | $N_1$ | 3616.9 | Brown mudstone | 40 | 17 | 14 | 7 | 17 | 1 | 3 | – | -4.44 | -8.57 | 61.78 | 113.94 |
| ES1 | $N_1$ | 3617.2 | Brown mudstone | 41 | 15 | 15 | 5 | 16 | 5 | 4 | – | -5.33 | -7.79 | 57.09 | 112.5 |
| ES1 | $N_1$ | 3618.1 | Brown mudstone | 40 | 16 | 14 | 8 | 16 | 3 | 4 | – | -4.85 | -9.37 | 66.72 | 112.7 |
| ES1 | $N_1$ | 3618.6 | Gray silty mudstone | 42 | 17 | 13 | 6 | 20 | 3 | 1 | – | -5.21 | -7.95 | 58.04 | 112.67 |
| ES1 | $N_1$ | 3619.1 | Brown silty mudstone | 39 | 16 | 13 | 7 | 19 | 3 | 3 | – | -5.75 | -10.57 | 74.37 | 110.26 |
| ES1 | $N_1$ | 3619.6 | Brown mudstone | 35 | 17 | 14 | 8 | 18 | 4 | 3 | – | -5.1 | -8.02 | 58.46 | 112.86 |
| ES1 | $N_1$ | 3620.1 | Brown mudstone | 41 | 14 | 12 | 6 | 21 | 3 | 2 | – | -4.84 | -7.82 | 57.27 | 113.49 |
| ES1 | $N_1$ | 3622.05 | Brown mudstone | 40 | 15 | 14 | 8 | 18 | 3 | 2 | – | -5.28 | -7.74 | 56.79 | 112.63 |
| ES1 | $N_1$ | 3622.1 | Brown mudstone | 43 | 15 | 12 | 10 | 18 | 1 | 2 | – | -4.94 | -9.34 | 66.53 | 112.53 |
| ES1 | $N_1$ | 3622.35 | Brown mudstone | 40 | 16 | 11 | 9 | 17 | 3 | 3 | – | -4.81 | -8.74 | 62.82 | 113.1 |
| ES1 | $N_1$ | 3622.9 | Brown mudstone | 42 | 16 | 15 | 8 | 15 | 1 | 3 | – | -4.7 | -7.54 | 55.61 | 113.92 |
| ES1 | $N_1$ | 3623.3 | Brown mudstone | 39 | 15 | 14 | 8 | 16 | 4 | 4 | – | -4.87 | -8.48 | 61.23 | 113.1 |
| ES1 | $N_1$ | 3624 | Brown mudstone | 41 | 15 | 13 | 8 | 18 | 3 | 2 | – | -4.37 | -9.08 | 64.92 | 113.83 |
| ES1 | $N_1$ | 3624.5 | Gray-brown pelitic siltstone | 41 | 11 | 8 | 8 | 30 | 2 | 1 | – | -5.12 | -9.94 | 70.32 | 111.86 |
| ES1 | $N_1$ | 3625 | Brown pelitic siltstone | 38 | 7 | 6 | 20 | 28 | 1 | 1 | – | -5.58 | -10.36 | 73.01 | 110.71 |
| ES1 | $N_1$ | 3625.5 | Brown mudstone | 42 | 14 | 12 | 7 | 17 | 5 | 3 | – | -4.62 | -7.58 | 55.85 | 114.06 |
| ES1 | $N_1$ | 3626.3 | Brown silty mudstone | 49 | 9 | 8 | 8 | 22 | 2 | 2 | – | -6.81 | -10.06 | 71.08 | 108.34 |
| ES1 | $N_1$ | 3627.1 | Brown mudstone | 40 | 17 | 12 | 8 | 17 | 3 | 3 | – | -4.57 | -8.61 | 62.03 | 113.65 |
| ES1 | $N_1$ | 3627.8 | Brown mudstone | 52 | 14 | 10 | 3 | 20 | 1 | 1 | – | -5.21 | -10.2 | 71.98 | 111.55 |
| ES1 | $N_1$ | 3628.6 | Brown pelitic siltstone | 44 | 11 | 8 | 14 | 21 | 1 | 1 | – | -5.84 | -9.07 | 64.85 | 110.82 |
| ES1 | $N_1$ | 3629.6 | Brown mudstone | 41 | 16 | 12 | 8 | 17 | 4 | 3 | – | -6.51 | -8.67 | 62.39 | 109.65 |
| ES1 | $N_1$ | 3629.8 | Brown mudstone | 38 | 11 | 9 | 22 | 18 | 1 | 1 | – | -5.51 | -9.5 | 67.54 | 111.28 |
| ES1 | $N_1$ | 3630.3 | Brown mudstone | 37 | 15 | 13 | 10 | 17 | 4 | 3 | – | -4.82 | -9.64 | 68.42 | 112.63 |
| ES1 | $N_1$ | 3631.1 | Brown mudstone | 41 | 15 | 12 | 11 | 17 | 1 | 3 | – | -4.88 | -7.26 | 53.97 | 113.69 |
| ES1 | $N_1$ | 3631.6 | Brown mudstone | 41 | 13 | 11 | 9 | 20 | 3 | 2 | – | -5.3 | -9.14 | 65.29 | 111.89 |
| ES1 | $N_1$ | 3632.1 | Brown mudstone | 45 | 13 | 10 | 8 | 19 | 2 | 2 | – | -4.42 | -7.37 | 54.61 | 114.58 |
| ES1 | $N_1$ | 3634.2 | Gray-brown mudstone | 38 | 21 | 18 | – | 16 | 5 | 2 | – | -4.63 | -6.31 | 48.52 | 114.68 |
| ES1 | $N_1$ | 3634.3 | Gray pelitic siltstone | 43 | 16 | 12 | – | 25 | 4 | 1 | – | -4.99 | -9.03 | 64.61 | 112.58 |
| ES1 | $N_1$ | 3635 | Brown mudstone | 38 | 16 | 13 | 13 | 16 | 1 | 3 | – | -5.65 | -7.07 | 52.87 | 112.21 |
| ES1 | $N_1$ | 3635.1 | Brown mudstone | 41 | 13 | 11 | 12 | 19 | 2 | 2 | – | -5.28 | -6.46 | 49.37 | 113.27 |

**Table 1** continued

| Well | Horizon | Depth (m) | Lithology | Quartz (%) | Chlorite (%) | Mica (%) | Calcite (%) | Plagiocla se (%) | Microcline(%) | Hematite (%) | Dolomite | $\delta^{13}C_{PDB}$ (‰) | $\delta^{18}O_{PDB}$ (‰) | t (°C) | Z |
|---|---|---|---|---|---|---|---|---|---|---|---|---|---|---|---|
| ES1 | N₁ | 3635.6 | Brown mudstone | 37 | 17 | 14 | 7 | 17 | 3 | 5 | – | –4.23 | –7.52 | 55.49 | 114.89 |
| ES1 | N₁ | 3636.1 | Dark gray siltstone | 37 | 9 | 6 | 17 | 22 | 4 | – | 4 | –4.61 | –8.12 | 59.06 | 113.81 |
| ES1 | N₁ | 3636.7 | Grayish-green pelitic siltstone | 20 | 8 | 6 | 47 | 15 | 1 | – | 3 | –5.81 | –5.38 | 43.36 | 112.72 |
| ES1 | N₁ | 3637.2 | Brown mudstone | 39 | 14 | 12 | 14 | 14 | 3 | 4 | – | –5.24 | –6.69 | 50.68 | 113.24 |
| ES1 | N₁ | 3637.9 | Grayish-green pelitic siltstone | 19 | 6 | 4 | 33 | 37 | 1 | – | – | –5.66 | –8.61 | 62.03 | 111.42 |
| ES1 | N₁ | 3638.7 | Brown mudstone | 34 | 12 | 11 | 23 | 15 | 3 | 2 | – | –4.66 | –9.17 | 65.47 | 113.19 |
| ES1 | N₁ | 3639.1 | Grayish-green silty mudstone | 23 | 7 | 6 | 54 | 9 | 2 | – | – | –5.87 | –9.49 | 67.47 | 110.55 |

Temperature and pressure increase with increased burial depth of sediments. As a consequence, $CO_2$ is generated by thermal decarboxylation of organic material. Its $\delta^{13}C$ values vary between −4.0 and −35.0 ‰ (Suess and Whiticar 1989). Organic acid and $CO_2$ dissolve easily in water generated by the dehydration of clay minerals during compaction (e.g., interlayer water, absorbed water, or constitution water). The resulting acidic solution can dissolve feldspar, lithic fragments, and carbonate cements to form secondary pores. Under the circumstances, the diagenetic environment is acidic with relatively strong oxidizing potential, with temperatures between 80 and 120 °C (Surdam et al. 1989).

Measured $\delta^{13}C$ of the carbonate cement samples varies between −6.8 and −4.0 ‰ (mean −5.0 ‰). The range is concentrated, and the average is near −4 ‰, so only a little effect comes from organic carbon. On the basis of the relationship between carbon and oxygen isotope compositions and salinity of the aqueous medium, Keith and Weber (1964) proposed an empirical formula to discriminate between marine limestone and freshwater limestone, and then to distinguish the formation environment. Z < 120 indicates freshwater limestone and Z > 120 indicates marine limestone. Z can be used to indicate ancient salinity (Zhang 1985; Fu 1996; Shao et al. 1996; Keith and Weber 1964), as follows.

$$Z = 2.048 \times (\delta^{13}C + 50) + 0.498 \times (\delta^{18}O + 50)$$

In the above formula, $\delta^{18}O$ and $\delta^{13}C$ values follow the PDB standard. The Z values of samples varied between 108.34 and 114.89 (mean 112.77); all of which were less than 120. This indicates that the diagenetic fluid of carbonate cement was mainly leaching freshwater and water in sediment.

Generally, $\delta^{18}O$ values appear negatively skewed along with increased burial depths (Wang 2000). $\delta^{18}O$ values of carbonate cement show close relationship with water temperature and decrease with increased temperature, when salinity remains unchanged. Shackleton (1974) proposed a formula to calculate ancient water temperature as follows.

$$t = 16.9 - 4.38(\delta c - \delta w) + 0.1(\delta c - \delta w)^2,$$

where t is the ancient water temperature for generating carbonate cement, δc is $\delta^{18}O$ of carbonate cement (PDB standard), and δw is $\delta^{18}O$ of ocean water (SMOW standard). The $\delta^{18}O$ of ancient ocean water can only be inferred. While (Jiang 1991) indicated that the $\delta^{18}O$ value of ancient ocean water was lower than contemporary ocean water and $\delta^{18}O$ (SMOW) was only 0 since the Pleistocene, Knauth, and Epstein (1976) postulated that the $\delta^{18}O$ value has been 0 (SMOW) since the Cambrian, suggesting that ancient ocean water is the same as modern. Muehlenbachs
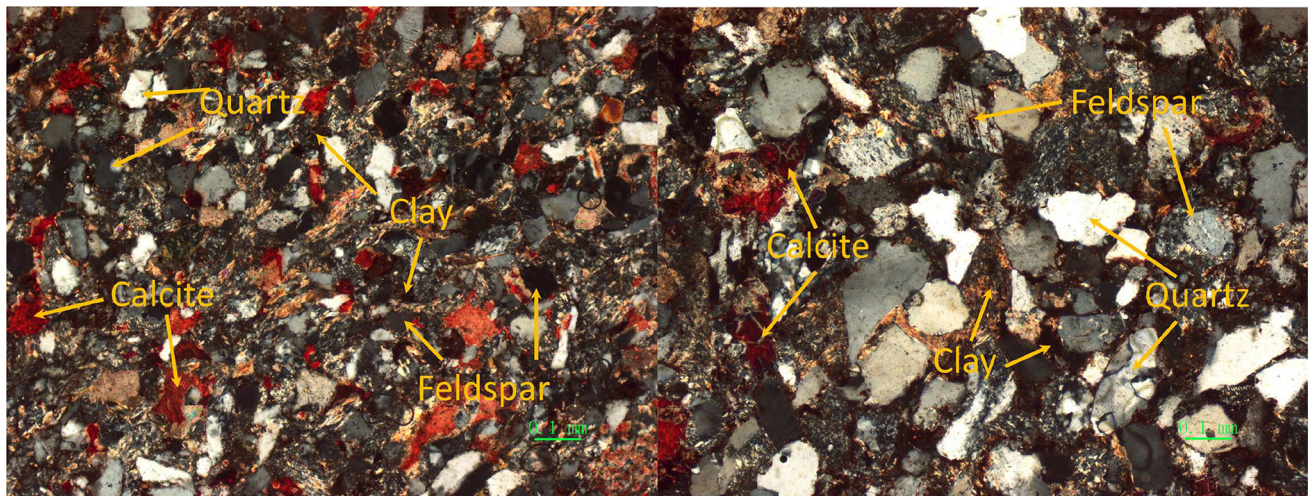
**Fig. 2** Characteristics of clay and calcite cement in feldspar sandstones of the Upper Ganchaigou Formation in the Eboliang III area. *Left figure* ES1, Upper Ganchaigou Formation (N1), 3990.70 m, fine feldspar sandstone with mainly clay cement and minor calcite cement

(+) ×100; *Right figure* ES1, Upper Ganchaigou Formation (N1), 3995.20 m, fine feldspar sandstone with mainly clay cement and minor calcite cement. Long mineral grains in directional alignment (+) ×100
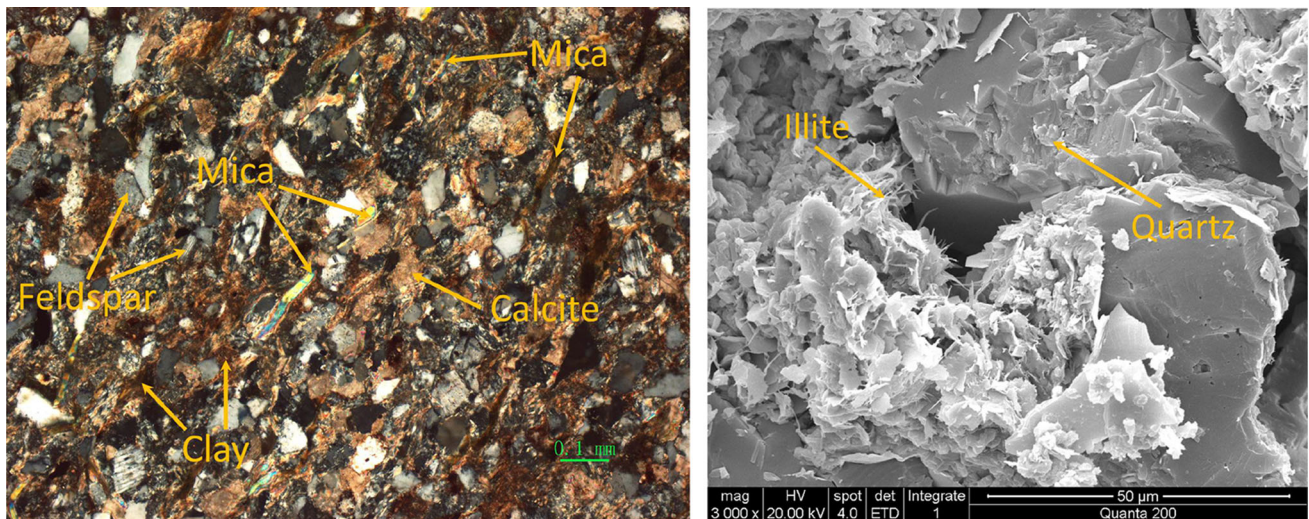


**Fig. 3** Characteristics of compaction and plastic deformation in Upper Ganchaigou Formation. *Left figure* ES1, Upper Ganchaigou Formation (N$_1$), 3995.20 m, fine feldspar sandstone with mainly clay cement and minor calcite cement. Long mineral grain in directional

alignment (+) ×100; *Right figure* ES1, Upper Ganchaigou Formation (N$_1$), 3995.20 m, sandstone. Quartz with III-order enlargement. Thread-like illite in residual intergrain pore

and Clayton (1972) agreed with this, suggesting that the $\delta^{18}O$ (SMOW) of ocean water during the entire Phanerozoic was $0 \pm 2$ ‰ as a result of the buffering from water–rock reactions. Although we cannot obtain the actual $\delta^{18}O$ value of ancient ocean water to use in calculating diagenetic temperature, we can apply the temperature formula to observe the relationship between $\delta^{18}O$ and diagenetic temperature, which should qualitatively distinguish higher or lower temperatures (Zhang 1985). We assumed the $\delta^{18}O$ (SMOW) of Miocene ocean water was 0 and used the carbonate cement carbon and oxygen isotope values to

reconstruct the Upper Ganchaigou Formation (Eboliang III structural belt) temperatures (Table 1). The samples have a maximum temperature of 77.84 °C, a minimum temperature of 44.36 °C, and a mean of 62.30 °C, but the actual temperature may be higher than the calculated temperature because of diagenetic influence. According to the petroleum and natural gas industry standards of The People's Republic of China (SY/T 5477-2003: The division of diagenetic stages in clastic rocks), the temperature range belongs to the B period of the early diagenesis stage or the A period of the middle diagenesis stage.
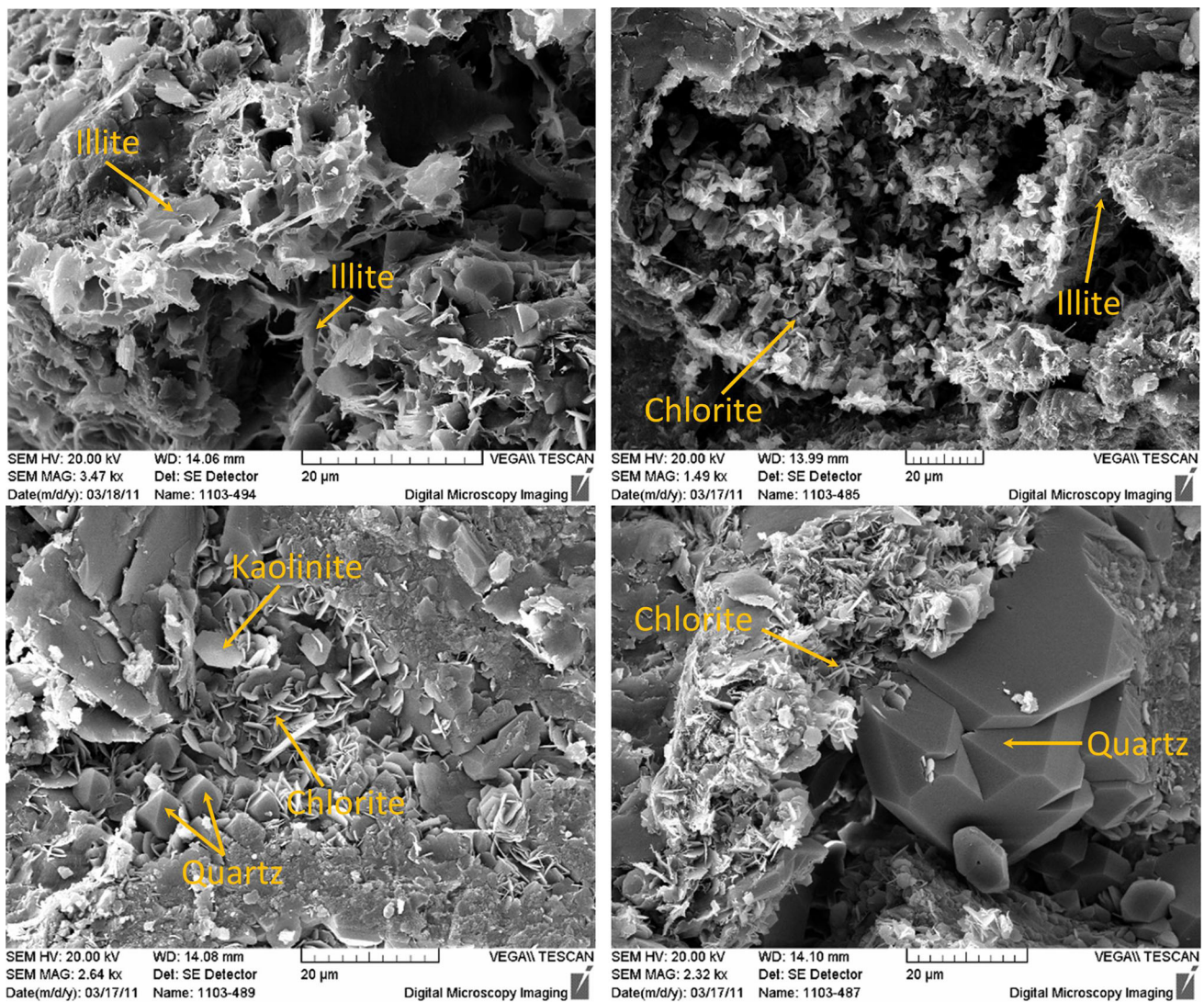
**Fig. 4** Micropore structures and clay minerals in the Upper Ganchaigou Formation. *Upper left figure* ES1, Upper Ganchaigou Formation (N1), 3990.56 m, siltstone. Thread-like illite developed on the surface of grains (×3470); *Upper right figure* ES1, Upper Ganchaigou Formation (N1), 3989.74 m, siltstone. Needle–leaf chlorite and thread-like illite developed in solution pores in grains (×1490); *Lower left figure* ES1, Upper Ganchaigou Formation (N1), 3989.74 m, siltstone. Thread-like illite developed on the surface of grains. Autogenetic quartz developed here (×2640); *Lower right figure* ES1, Upper Ganchaigou Formation (N1), 3989.74 m, siltstone. Needle–leaf chlorite developed on the surface of grains. Quartz with III-order enlargement (×2320)

## Major elements

The effects of natural environments on decomposition, migration, and enrichment of various elements are different, so content variations can be used to a certain extent to infer transitions of sedimentary environments. The oxides of common elements such as $CaO$, $MgO$, $K_2O$, $Na_2O$, $SiO_2$, $Al_2O_3$, $Fe_2O_3$, and $TiO_2$ are sensitive to environmental change and are significant environmental indicators (Zhong et al. 1998; Kuang et al. 2002). The distribution ratios of various elements in rock strata are affected by physicochemical properties as well as ancient climate and environment. Therefore, distributions and inter-element ratio variations of trace elements indicate the evolution of the ancient environment to some degree (Wang et al. 1997; Song 2005). According to previous studies (Wang 1993; Xi et al. 1998), high $CaCO_3$ content in strata that formed in the early stage of chemical deposition indicates an arid climate, while low content indicates a humid climate. Major element oxides ($CaO$, $MgO$, $K_2O$, $Na_2O$, $SiO_2$, $Al_2O_3$, and $Fe_2O_3$) show obvious relationships in sample analytical results (Table 3). Amplitude of variation is large between 3640 and 3636 m but tends to be smooth and stable above 3635 m. $CaO$ content is high in the early stage of deposition, indicating an arid climate. Terrigenous debris input is small and evaporation capacity is large. Content of $CaO$

**Table 2** X-ray diffraction analysis of Upper Ganchaigou Formation in Eboliang III area

| Well | Depth | Horizon | Lithology | Relative content of clay mineral (%) | | | | Mixed-layer ratio (% S) | | Clay mineral (%) |
|------|-------|---------|-----------|------|------|------|------|------|------|------|
| | | | | I/S | I | K | C | I/S | C/S | |
| ES1 | 3617.55 | N$_1$ | Brown sandy mudstone | 6 | 71 | 7 | 16 | 25 | – | 40.8 |
| ES1 | 3622.46 | N$_1$ | Brown sandy mudstone | 11 | 67 | 7 | 15 | 35 | 912 | 50.2 |
| ES1 | 3623.73 | N$_1$ | Brown sandy mudstone | 9 | 71 | 7 | 13 | 35 | 913 | 50.5 |
| ES1 | 3624.15 | N$_1$ | Brown sandy mudstone | 15 | 66 | 6 | 13 | 35 | 914 | 48.1 |
| ES1 | 3624.9 | N$_1$ | Brown sandy mudstone | 13 | 68 | 6 | 13 | 35 | 915 | 45.7 |
| ES1 | 3625.8 | N$_1$ | Brown sandy mudstone | – | 78 | 7 | 15 | – | – | 11.3 |
| ES1 | 3626.7 | N$_1$ | Brown sandy mudstone | 11 | 71 | 6 | 12 | 35 | 916 | 31.4 |
| ES1 | 3626.81 | N$_1$ | Brown sandy mudstone | 16 | 65 | 7 | 12 | 35 | 917 | 33.0 |
| ES1 | 3628.94 | N$_1$ | Brown sandy mudstone | 14 | 65 | 8 | 13 | 30 | 918 | 31.4 |
| ES1 | 3631.23 | N$_1$ | Brown sandy mudstone | 7 | 72 | 6 | 15 | 30 | – | 54.7 |
| ES1 | 3631.64 | N$_1$ | Brownish gray pelitic siltstone | 21 | 61 | 7 | 11 | 30 | 919 | 25.3 |
| ES1 | 3634.38 | N$_1$ | Brownish gray pelitic siltstone | 12 | 64 | 10 | 14 | 30 | 920 | 40.0 |
| ES1 | 3635.13 | N$_1$ | Brownish gray pelitic siltstone | 15 | 66 | 6 | 13 | 35 | 921 | 35.5 |
| ES1 | 3636.08 | N$_1$ | Gray pelitic siltstone | 18 | 61 | 8 | 13 | 40 | 922 | 34.3 |
| ES1 | 3637.48 | N$_1$ | Gray pelitic siltstone | 11 | 69 | 7 | 13 | 35 | 923 | 42.3 |
| ES1 | 3989.6 | N$_1$ | Gray siltstone | 13 | 75 | – | 12 | 7 | – | 25.4 |
| ES1 | 3989.64 | N$_1$ | Gray siltstone | 12 | 68 | 7 | 13 | 35 | 924 | 22.7 |
| ES1 | 3990.7 | N$_1$ | Gray siltstone | 12 | 68 | 7 | 13 | 35 | 926 | 24.6 |
| ES1 | 3990.7 | N$_1$ | Gray siltstone | 31 | 56 | – | 13 | 7 | – | 21.4 |
| ES1 | 3991.13 | N$_1$ | Gray siltstone | 12 | 68 | 7 | 13 | 35 | 927 | 29.4 |
| ES1 | 3991.2 | N$_1$ | Gray siltstone | 18 | 68 | – | 14 | 6 | – | 36.9 |
| ES1 | 3993.66 | N$_1$ | Brown mudstone | 8 | 70 | 7 | 15 | 25 | – | 53.5 |
| ES1 | 3994.94 | N$_1$ | Gray siltstone | 59 | 16 | 15 | 10 | 60 | 928 | 37.0 |
| ES1 | 3995.23 | N$_1$ | Gray siltstone | 20 | 70 | – | 10 | 8 | – | 23.2 |
| ES1 | 3995.7 | N$_1$ | Gray siltstone | 20 | 68 | – | 12 | 6 | – | 27.2 |

Standard: SY/T 5163-1995. The reason that S + I/S + I + K + C + C/S = 101 or 99 is rounded numbers rather than data bias. Clay mineral with mixed-layer ratio greater than 70 % is smectite. Where S is smectite, I/S is illite/smectite mixed layer, I is illite, K is kaolinite, C is chlorite, and C/S is chlorite/smectite mixed layer. Mixed-layer ratio, 20 % for example, means the ratio between illite and smectite or chlorite and smectite is 20

decreased in the late stage of deposition, indicating a humid climate. In this period, terrigenous debris input increased and evaporation capacity decreased, therefore decreasing salinity. The climate of the Upper Ganchaigou Formation changed frequently in the early stage of deposition, indicated by the significant change in oxide content. Climate changed a little in the late stage which is indicated by the stable oxide contents. The environment of enriched $Ca^{2+}$ formation was drier than the environment of enriched $Mg^{2+}$ formation, because the transfer ability of $Ca^{2+}$ is greater than that of $Mg^{2+}$ as a result of its larger ionic radius (Kuang et al. 2002). In lacustrine sediments without seawater intrusion, Sr/Ba > 1 indicates that lake water had started alkalization, while Sr/Ba < 1 indicates that lake water was still fresh (Zhong et al. 1998; Kuang et al. 2002; Wang et al. 1997; Song 2005). Only three samples in the

lower section of the Upper Ganchaigou Formation present a Sr/Ba ratio greater than 1. Salinity varied greatly but was mainly fresh–brackish water in the early stage, and was mainly fresh in the late stage.

Lake carbonate is a recognized indicator of ancient climate and environment (Wang and Li 1991). With a warmer provenience climate, chemical weathering becomes more intense and the carbonate content of the lake reduces due to leaching loss of allogenic carbonate and CaO. Carbonate does not migrate downward after deposition (Chen 1995). The ratios of soluble and stable compounds, like that of carbonate and $Al_2O_3$, can be used to infer the extent of weathering crust loss and then to indicate climate variation during deposition. The decrease in eluviation coefficient indicates a warmer and wetter climate with more intense chemical weathering (Ковда 1981; Yang

**Table 3** Characteristics of major elements and trace elements in the Upper Ganchaigou Formation in the Eboliang III area



**Table 4** Mineral characteristics of the Upper Ganchaigou Formation in Eboliang III Area
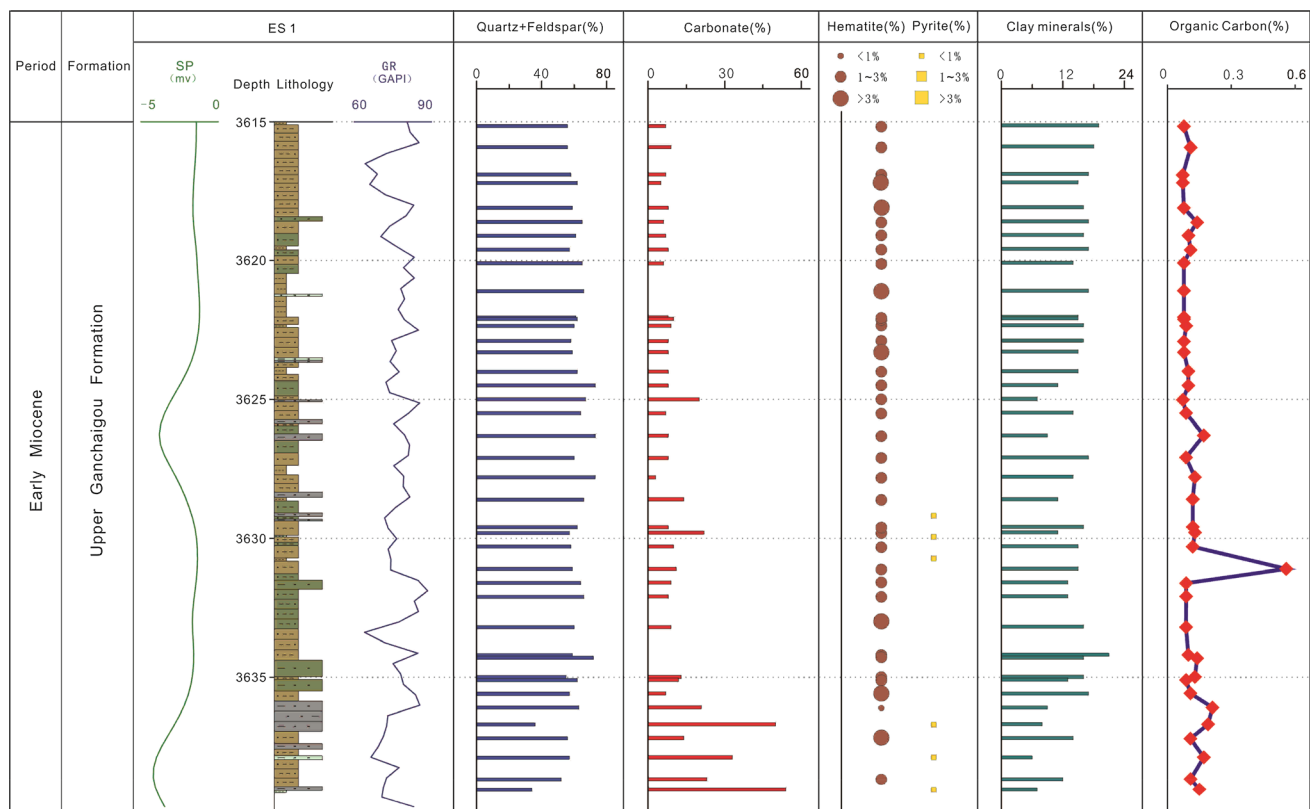


and zhang 1998). Carbonate content is higher in the early stage and lower in the late stage (Table 4). The variations of carbonate content indicated that the climate was dry and cold in the early stage of the Upper Ganchaigou Formation, and warm and humid in the late stage of the Upper Ganchaigou Formation.

## Conclusions

Calcite is the main carbonate cement in the Upper Ganchaigou Formation, and only a small amount of dolomite was found. Particles in sandstone exhibited mainly point-line contacts and many plastic lithic fragments or micas

show directional alignment. Clays are abundant, with means up to 35.03 %, and mainly consist of illite, chlorite, and mixed-layer illite–smectite. On the basis of diagenetic characteristics of clay minerals and carbonate cements, the diagenetic stage of the Upper Ganchaigou Formation is regarded as the B period of the early diagenesis stage or the A period of the middle diagenesis stage. Carbon and oxygen isotope compositions of carbonate cement present $\delta^{13}C$ values that range between $-6.8$ and $-4.0$ ‰ (mean $-5.0$ ‰) and $\delta^{18}O$ values that range between $-11.1$ and $-5.4$ ‰ (mean $-8.7$ ‰). The calculated ancient salinity Z values were distributed between 108.34 and 114.89 (mean 112.77), and the formation temperature of carbonate cement was between 43.36 and 77.84 °C (mean 62.30 °C).

According to analysis of measured result of major elements, trace elements, and content of organic carbon, major elements appeared obvious in correlation with others, and varied regularly from the early to late stages of the Upper Ganchaigou Formation. Climate of the Upper Ganchaigou Formation changed frequently in the early stage. Climate was dry and cold in the early stage of the Upper Ganchaigou Formation, and warm and humid in the late stage.

# References

Abdel-Wahab A, McBride EF (2001) Origin of giant calcite-cemented concretions, Temple Member, Qasr El Sagha Formation (Eocene), Faiyum depression, Egypt. J Sediment Res 71(1):70–81

Boles JR (1998) Carbonate cementation in Tertiary sandstones, San Joaquin Basin, California [M]. Wiley, New York 261–284

Cai GQ, Guo F, Liu XT, Sui SL (2009) Carbon and oxygen isotope characteristics and Palaeoenvironmental implications of lacustrine carbonate rocks from the Shahejie Formation in the Dongying sag. Earth Environ 37(4):347–354

Chen ZL (1995) The records of characteristics of early lithogenous change in Yungui tableland lake carbonate [C]//Geomorphology and Quaternary Studies, GSC. Physiognomy Environment Development. Chinese Environment & Science Press, Beijing, p 79

Chen SL, Luo Q (2004) Fault development characteristics and hydrocarbon accumulation in the west section of the northern fringe of Qaidam Basin. Nat Gas Ind 24(3):22–25

Chen J, Xie M, Shi JA, Zhang YS, Sun GQ, Wu ZX, Wang GC (2011) Reservoir characteristics of Xiaganchaigou formation in Mabei area of Northern Qaidam Basin. Nat Gas Geosci 22(5):821–826

Dong FX, Liu L, Ma YP (2004) Carbon and oxygen isotopes of calcite cement in the lower part of the Sha-1 Formation, the Dagang beach area. Pet Geol Exp 26(6):590–593

Fayek M, Harrison TM, Grove M, Mckeegan KD, Coath CD, Boles JR (2001) In situstable isotopic evidence for protracted and complex carbonate cementation in a petroleum reservoir, North Coles Levee, San Joaquin Basin, California, USA. J Sediment Res 71(3):444–458

Friedman I, O'Neil JR (1977) Compilation of stable isotope fractionation factors of geochemical interest[M]‖Fleisher M Data of Geochemistry. 6th ed. Reston, Virginia, USGS, p 60

Fu QL (1996) Relationships between carbon and oxygen isotopic compositions and diagenetic environments of Lower Tertiary carbonate on the northwestern margin of Kuqa Basin, Xinjiang. J Stratigr 20(4):280–283

Guo ZQ, Sun P, Xu ZY, Zhang L, Zhang SS, Tian JX (2011) Controlling factors of Quaternary lithologic gas reservoirs in the Sanhu area, Qaidam Basin. Acta Pet Sin 32(6):985–990

Huang SJ, Shi H, Zhang M, Shen LC, Wu WH (2002) Application of strontium isotope stratigraphy to diagenesis research. Acta Sedimentol Sin 20(3):359–366

Hudson JD (1977) Stable isotopes and limestone lithification. J Geol Soc 133(6):637–660

Jiang JJ (1991) Palaeoclimates on the upper Yangtze platform during the early Carboniferous. Sediment Geol Tethyan Geol 3:40–45

Keith ML, Weber JN (1964) Isotopic composition and environmental classification of selected limestones and fossils. Geochim Cosmochim Acta 28:1787–1816

Knauth LP, Epstein S (1976) Hydrogen and oxygen isotope ratios in nodular and bedded cherts. Geochim Cosmochim Acta 40(9):1095–1108

Kuang SP, Xu Z, Zhang SS, Ma ZD (2002) Applying geochemistry to research into Meso-Cenozoic climate: discussion on Jurassic climatic change in Sichuan Basin, China. J Qingdao Inst Chem Technol 3(1):4–9

Li FJ, Liu Q, Liu DH, Qi WZ (2009) Characteristics and influential factors of Low-Ganchaigou formation reservoir in north edge of Qaidam Basin. Nat Gas Geosci 20(1):44–49

Liu DL, Sun XR, Li ZS, Tang NA, Tan Y, Liu B (2006) Analysis of carbon and oxygen isotope on the Ordovician dolostones in the Ordos Basin. Pet Geol Exp 28(2):155–161

Liu W, Lin CY, Wang GM, Liu J, Jiang YB (2009) Characteristics of low-permeability reservoir and its origin in Youquanzi oilfield in the north west part of Qaidam Basin. Acta Pet Sin 30(3):417–421

Macaulay CI, Haszeldine RS, Fallick AE (1993) Distribution, chemistry, isotopic composition and origin of diagenetic carbonates: magnus sandstone, North Sea. J Sediment Pet 63(1):33–43

McBride EF, Parea GC (2001) Origin of highly elongate, calcite-cemented concretions in some Italian coastal beach and dune sands. J Sediment Res 71(1):82–87

Muehlenbachs K, Clayton RN (1972) Oxygen isotope geochemistry of submarine. Can J Earth Sci 9(5):471–478

Ortoleva PJ (1994) Basin Compartments and Seals, AAPG Memoir 61 [M]. AAPG Press, Tulsa, p 477

Rosenbaum J, Sheppard SMF (1986) An isotopic study of siderites, dolomites, and ankerites at high temperature. Geochim Cosmochim Acta 50(6):1147–1150

Rossi C, Marfil R, Ramseyer K, Permanyer A (2001) Facies-related diagenesis and multiphase siderite cementation and dissolution in the reservoir sandstones of the Khatatba Formation, Egypt's western desert. J Sediment Res 71(3):459–472

Shackleton NJ (1974) Attainmnet of isotopic equilibrium between ocean water and benthonic foraminifera genus Uvigerina: isotopic changes in the ocean during the last glacial. Colloq Int CNRS 219:203–209

Shao LY, Dou JW, Zhang PF (1996) Paleogeographic significances of carbon and oxygen isotopes in Late Permian rocks of southwest China. Geochimica 25(6):575–580

Song MS (2005) Sedimentary environment geochemistry in the Shasi Section of Southern Ramp, Dongying depression. J Mineral Petrol 5(1):67–73

Suess E, Whiticar MJ (1989) Methane-derived $CO_2$ in pore fluids expelled from the Oregon subduction zone. Palaeogeogr Palaeoclimatol Palaeoecol 71(1):119–136

Sun YS, Shen YM, Xu X, Yang F (2002) Evaluating and predicting heterogeneous reservoirs and its oil-bearing properties by the analysis technique of the diagenetic lithofacies: taking Hadexun area in Tarim Basin as an example. Acta Sedimentol Sin 20(1):55–59

Sun GQ, Xie M, Zhang YS, Zhao MJ, Kang J, Shi JA (2011) Sedimentary characteristics and evolution of Paleogene lower Xiaganchaigou Formation in northern Mahai area, northern margin of Qaidam Basin. Lithol Reserv 23(6):56–61

Sun GQ, Ma JY, Wang HF, Chen J, Zhang YS, Jia YY, Zhang SY, Shi JA (2012) Characteristics and significances of carbonate cements in northern Mahai region, northern margin of Qaidam Basin. Pet Geol Exp 34(2):134–139

Surdam RC, Crossey LJ, Hagen ES (1989) Organic-inorganic interactions and sandstone diagenesis. AAPG Bull 73(1):1–23

Wang YF (1993) Lacustrine carbonate chemical sedimentation and climatic-environmental evolution—a case study of Qinghai Lake and Daihai Lake. Oceanol et Limnol Sin 24(1):31–35

Wang DR (2000) Geochemistry of stable isotopes in oil and gas [M], Petroleum Industry Press, Beijing, pp 137–196

Wang SM, Li JR (1991) Lake sediments—an effect mean of research for palaeoclimate. Chin Sci Bull 36(1):54–56

Wang SJ, Huang XZ, Tuo JC, Shao HS, Yan CF, Wang SQ, He ZR (1997) Evolutional characteristics and their Paleoclimate significance of trace elements in the Hetaoyuan Formation, Biyang Depression. Acta Sedimentol Sin 15(1):65–70

Wang JC, Liu P, Ni JL, Chen L, Cao HF, Wan FL (2007a) Effects of deformation partitioning on hydrocarbon migration-accumulation in the northern margin of Qaidam Basin. Acta Pet Sin 28(3):27–31

Wang Q, Zhuo XZ, Chen GJ, Li XY (2007b) Characteristics of carbon and oxygen isotopic compositions of carbonate cements in Triassic Yanchang sandstone in Ordos Basin. Nat Gas Ind 27(10):28–32

Wang Q, Hao LW, Chen GJ, Zhang GC, Zhang R, Ma XF, Wang H (2010) Forming mechanism of carbonate cements in siliciclastic sandstone of Zhuhai Formation in Baiyun sag. Acta Pet Sin 31(4):553–558

Xi XX, Mu DF, Fang XM, Li JJ (1998) Climatic change since the Late Miocene in west China evidence from anion chlorine in the Linxia Red Basin. Acta Sedimentol Sin 16(2):155–160

Xiao AC, Chen ZY, Yang SF, Ma LX, Gong QL, Chen YZ (2005) The study of Late Cretaceous paleostructural characteristics in northern Qaidam Basin. Earth Sci Front 12(4):451–457

Xie QB, Guan SR (2000) Sedimentary facies type and reservoir evaluation for the northern Qaidam Basin. Pet Explor Dev 27(2):40–44

Yan CF, Yuan JY, Chen QL, Shao HS, Zhang ZG (2011) Discovery of the high-quality source rock of the first member of Dameigou Formation in the east part of the northern Qaidam Basin. Acta Pet Sin 32(1):49–53

Yang WL, Zhang QS (1998) Geochemical characteristics and its climatic significance in the borecore AB-32 from Ikroavik lake in the Tundra barrow, Arctic Alaska. Chin J Polar Res 10(4):351–360

Zhang XL (1985) Relationship between carbon and oxygen stable isotope in carbonate rocks and paleosalinity and paleotemperature of seawater. Acta Sedimentol Sin 3(4):17–28

Zhang J, He Z, Xu HB, Ji CH, Yuan Q, Shi JA, Lu XC (2012) Petrological characteristics and origin of permian Fengcheng formation dolomitic rocks in Wuerhe-Fengcheng Area, Junggar Basin. Acta Sedimentol Sin 30(5):859–867

Zhong W, Fang XM, Li JJ, Zhu JJ (1998) The geochemical record of paleoclimate during about 7.0–0.73 Ma in Linxia Basin, Gansu province. J Arid Land Resour Environ 12(1):36–43

Zhu YM, Zheng X, Liu XS, Zhang ZW (2007) Stable carbon isotope of authigenetic calcite used in reservoirs to tracing the hydrocarbon migration. Nat Gas Ind 27(9):24–27

Ковла ВА (1981) Soil science principle [M]. Translated by Lu BS, Zhou LK, Li YS (eds) Science Press, Beijing, p 132